

Nonlinear Phononic Control and Emergent Magnetism in Correlated Titanates

Mingqiang Gu and James M. Rondinelli*

*Department of Materials Science and Engineering,
Northwestern University, Evanston, IL 60208, USA*

Optical control of structure-driven magnetic order offers a platform for magneto-optical terahertz devices. We report how to control magnetic states in d^1 Mott insulating titanates using nonlinear phononics to transiently perturb the atomic structure based on density functional theory (DFT) calculations and solutions to a lattice Hamiltonian including nonlinear multi-mode interactions. We show that magnetism is tuned by indirect excitation of a Raman-active phonon mode, which controls the amplitude of the TiO_6 octahedral rotations and coupled static Ti–O Jahn-Teller distortions, through the infrared-active phonon modes of LaTiO_3 and YTiO_3 . The mode excitation reduces the rotational angle, driving a magnetic phase transition from ferromagnetic (FM) to A -type antiferromagnetic (AFM), and finally a G -type AFM state. This novel A -AFM state arises from a change in the exchange interactions and is absent in the bulk equilibrium phase diagram, but it emerges as a dynamically accessible optical-induced state. Our work shows nonlinear phononic coupling is able to stabilize phases inaccessible to static chemical pressure or epitaxial strain.

Recent advances in laser sciences enable light pulses to selectively pump phonon modes in crystals as a means to manipulate the transient atomic structure and structure-derived properties of materials. Ultrafast phononic control provides an alternative route beyond static methods, i.e. chemical pressure and thin film strain, to access nonequilibrium states [1]. By exciting an infrared-active (IR) mode so intensively that it induces a displacive force to a Raman mode through a nonlinear phononic (NLP) interaction, the charge-ordering state in manganites has been melted [2], the superconducting temperature in cuprate and fullerene systems has been increased [3, 4], and the direction of the electric polarization in a ferroelectric has been flipped [5]—all processes on the picosecond time scale. Recent work has also shown that a two-mode excitation approach may be used to control the direction of a targeted distortion using polarized light [6], broadening the prospect of ultrafast structural manipulation.

In addition to well-defined electronic and dielectric states, the magnetic order in complex transition metal oxides are exceedingly sensitive to subtle changes in atomic structure. Indeed, control over atomic structure through strain engineering or compositional changes can produce new ferroic states in manganites [7, 8], ruthenates [9], and titanates [10]; however, structure-induced magnetic phase transitions in complex ternary oxides remain to be designed using NLP control, i.e. magnetophononics [11, 12], deriving a new research branch called dynamical multiferroics [13, 14]. The main concept is to use light to exploit the structure-magnetic state dependencies originating in microscopic metal-oxygen-metal bond angles and metal-oxygen bond lengths [15]. In this sense, effective magnetic fields can be elicited through pure phononic excitation [16].

In this work, we demonstrate a protocol to manipulate the magnetic order in ternary oxides through ultrafast dynamical structure control. The prerequisite for such control relies on selection of an equilibrium material with

its magnetism dependent upon a cooperative atomic displacements, e.g. rotations of octahedra, that resemble a natural Raman-active mode of the crystal. The sensitivity of the phase stability is assessed through local perturbations to the atomic structure, and then the Raman mode that most resembles the local atomic distortion is targeted for mode-selective pumping through the NLP interactions. We demonstrate this process for the Mott insulating titanates and show that the NLP interactions provide access to both ferromagnetism (FM) and antiferromagnetism (AFM), including an layered A -type AFM absent from the equilibrium titanate phase diagram. Although this phase has been theoretically [17] predicted to be accessible with strain engineering, it remains to be observed in experiment and may be easier to achieve dynamically than through static methods. Finally, we show the critical laser intensity to drive the transitions can be tuned with thin film epitaxy, motivating nonlinear magnetophononic experiments on thin film titanates.

Ultrafast phononic structure control arises from the nonlinear terms in the Hamiltonian expressed as a function of the amplitudes of a Raman-active (A_g) and an IR-active phonon (B_u) mode [18]:

$$E = \frac{1}{2}\nu_R^2 Q_R^2 + \frac{1}{2}\nu_{IR}^2 Q_{IR}^2 + \frac{1}{3}a_3 Q_R^3 + \frac{1}{4}b_4 Q_{IR}^4 + g Q_R Q_{IR}^2, \quad (1)$$

where $\nu_{R,IR}$ and $Q_{R,IR}$ are the frequencies and amplitudes of the Raman and IR modes, respectively. The vibrational center of the Raman mode, which strongly affects macroscopic properties in complex oxides owing to changes in bond angles and lengths, is displaced by the IR mode through the nonlinear term $\sim Q_R Q_{IR}^2$. By coherently pumping the IR mode one is able to manipulate material properties on an ultrafast 10 ~ 100 picosecond timescale.

Titanates with one electron occupying the d orbital (d^1) are a model system to explore complex structure-

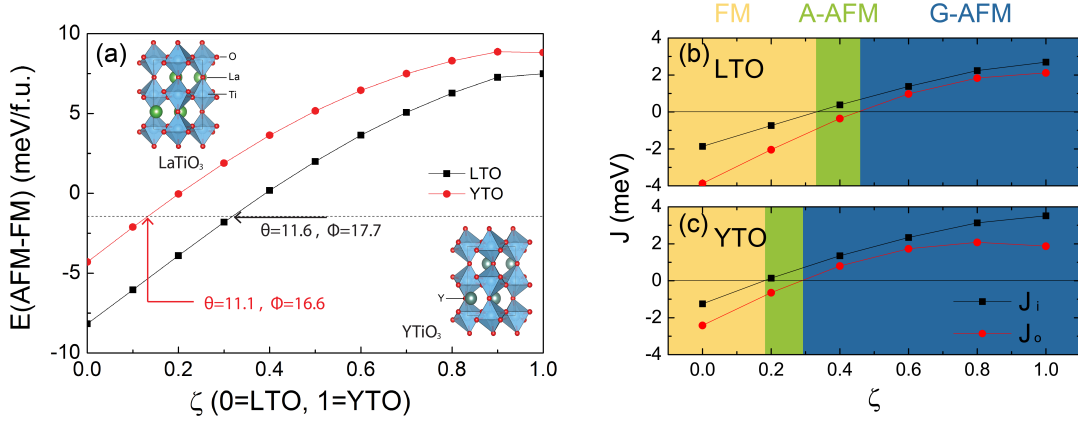


FIG. 1. (Color online) (a) Energy difference between FM and G-AFM phase as a function of ζ . (b) and (c) The exchange coupling constants between nearest in-plane (J_i) and out-of-plane (J_o) Ti atoms as functions of ζ in LTO and YTO. Different colors in (b) and (c) denote the magnetic ordering phase transition. The insets in (a) show the structure of LTO and YTO.

dependent electronic and magnetic properties [19]. Both LaTiO_3 and YTiO_3 are Mott insulators in this family [20]; however, they exhibit different magnetic [21, 22] and orbital [19, 23] ordered states. The ground state of LaTiO_3 (LTO) is a G -type antiferromagnet (AFM) with the Néel temperature $T_N = 150$ K whereas YTiO_3 (YTO) is an unusual ferromagnetic (FM) insulator with a Curie temperature of $T_C = 30$ K. The appearance of both FM and AFM spin configurations indicates the d^1 system is not a simple Mott insulator. Prior theoretical studies have reproduced the correct magnetic ground state [24–26] and identified it to be related to the lifting of the $3d - t_{2g}$ orbital degeneracy, which is correlated to the amplitude of the in-phase and out-of-phase TiO_6 octahedral rotations [19]. Such octahedral rotations are enhanced in YTO owing to the small Y cation size. The magnetic ordering has been theoretically shown to be tunable with strain [27]; however, there is no experimental observation reported. Importantly, A -type AFM has not been realized in any known d^1 titanate with a trivalent A site cations.

We first analyzed the relationship between the orthorhombic structure parameters and the magnetic order using first-principles calculations based on density functional theory (DFT) [28]. Both LTO and YTO exhibit $Pbnm$ symmetry whereby neighboring TiO_6 octahedra rotate about the c axis in-phase (c^+) and tilt in an out-of-phase sense about the pseudocubic $[110]$ direction (a^-a^- tilt pattern). The tilting (ϕ) and the rotational (θ) angles are defined as $\phi = (180^\circ - \angle(\text{Ti} - \text{O} - \text{Ti}))/2$, and $\theta = (90^\circ - \angle(\text{O} - \text{O} - \text{O}))/2$, where the $\text{Ti}-\text{O}-\text{Ti}$ and interoctahedral $\text{O}-\text{O}-\text{O}$ (denoted OOO) angles reported here follow the convention introduced in Ref. 29. Our calculated structure parameters for both titanates are in good agreement with the experimental data [28].

Because Y exhibits a smaller cation radius than La, the unit cell volume for YTO is 8% smaller than that of LTO. One consequence of this is that the Goldschmidt

tolerance factor $\tau = (r_A + r_O)/[\sqrt{2}(r_B + r_O)]$ is smaller for YTO than LTO (and both are smaller than 1). Thus, the rotation and tilt angles in YTO are larger than in LTO. The change in magnitude of the octahedral rotation amplitudes in the equilibrium structures affects the effective exchange coupling between neighboring Ti ions through superexchange interactions. If the total exchange coupling for nearest neighbors is expressed as $J = J_0 + J_{\text{SX}}$, where $J_0 > 0$ is the direct exchange coupling between two ions and J_{SX} is the superexchange between the two Ti ions bridged by an oxide ion, then according to the Goodenough-Kanamori-Anderson rules, J_{SX} should be negative for the d^1 system. This interaction then stabilizes an AFM spin configuration. Furthermore, the magnitude of superexchange $|J_{\text{SX}}| \propto (1 - \cos \angle(\text{Ti} - \text{O} - \text{Ti}'))$, decreases as the $\angle(\text{Ti} - \text{O} - \text{Ti}')$ deviates from 180° . Therefore when the rotational distortions increase, the spin system will favor FM spin order, and vice versa. These aforementioned exchange dependencies on the octahedral rotation angles is at the origin of the equilibrium magnetic phases in LTO and YTO.

To validate the structural origin of the magnetic configurations, we performed DFT calculations on hypothetical structures that follow an adiabatic trajectory connecting the LTO and YTO structures. Along this trajectory both chemical compositions are used to compute the difference in total energy between the known FM and G -AFM spin orders (Figure 1a). Formally, we define ζ as the independent structural parameter in the trajectory, such that $\zeta = 0$ ($\zeta = 1$) denotes the equilibrium LTO (YTO) structure. Structures between $\zeta = 0$ and 1 are obtained as a linear interpolation between the two end members, i.e. $x_\zeta(i) = x_0(i) + \zeta dx(i)$, in which $x(i)$ is the fractional coordinate for atom i and $dx(i) = x_1(i) - x_0(i)$. We find for both compounds that independent of the La or Y chemistry, if the titanate exhibits the LTO crystal structure ($\zeta = 0$) then the G -AFM state is always favored. As

ζ increases away from 0 in the LTO structure towards that of YTO, a magnetic transition occurs at $\zeta = 0.2$ for Y and $\zeta = 0.4$ for La; at these values the FM state becomes energetically favored.

Microscopically, these changes in magnetic states are due to changes in the effective exchange coupling J . To identify the different contributions from the rotation and tilt distortions, which are related to the equatorial or apical oxide anions atoms connecting the two Ti cations, respectively, we computed the in-plane (J_i) and out-of-plane (J_o) exchange constants between nearest Ti sites (Figure 1b). It is clear that the signs for both J_i and J_o change from negative (AFM coupling) to positive (FM coupling) as the structure evolves from that of LTO to YTO. The critical ζ for the in-plane coupling is about 0.2 while that for the out-of-plane is ~ 0.3 , which is consistent with the phase diagram in Figure 1. Remarkably, our analysis shows that there should be an additional A-type AFM phase bridging the FM and G-AFM phases in the region of $0.2 < \zeta < 0.3$. The total energy for the A-AFM configuration at $\zeta = 0.25$ is about 0.5 meV more stable than that of the FM phase.

The critical rotation and tilt angles required to achieve the transition (specified in the inset) are smaller than the average structure ($\zeta = 0.5$): In YTO these angles are $\theta = 11.1^\circ$, $\phi = 16.6^\circ$, which are close to those of LTO ($\theta = 11.6^\circ$, $\phi = 17.7^\circ$). Therefore, we propose that control of the magnetic state in the d^1 titanates should be possible through changes in the TiO_6 octahedral rotation and tilt angles. Since these rotational modes transform as the fully symmetric irreducible representation of the point group mmm , the next task is to identify the Raman mode that is optimally suited for optical pumping.

Using YTO as an example, we identify the Raman mode that most effectively modulates the octahedral rotation amplitude by computing the lattice dynamical properties of YTO and check the mode similarity among the seven Raman-active A_g modes with pure octahedral rotation, tilt and Jahn-Teller distortions [28]. The A_g mode (index no. 25, $\nu = 298 \text{ cm}^{-1}$) exhibits the largest composition of octahedral rotation. We find that variation in the amplitude of this Raman mode leads to changes in the octahedral rotational angle of $\partial\phi/\partial Q = 1.8^\circ/\text{\AA}\sqrt{\text{amu}}$. Furthermore, the energy difference $\Delta E(\text{AFM}-\text{FM})$ drops rapidly when this mode is excited (shown in Figure S1 of Ref. 28), which confirms our selection of this mode to tune the magnetic order.

Next, we identify which IR mode will most effectively couple to this A_g Raman mode through a NLP interaction. According to the theory of ionic Raman scattering, the amplitude of the Raman mode is largest when the frequency difference is between the driven Raman mode and the pumped IR mode is maximized [30]. Therefore the coherently pumped IR mode should be a high frequency mode albeit accessible to current laser THz-laser sources. The nonlinear coupling interactions between the

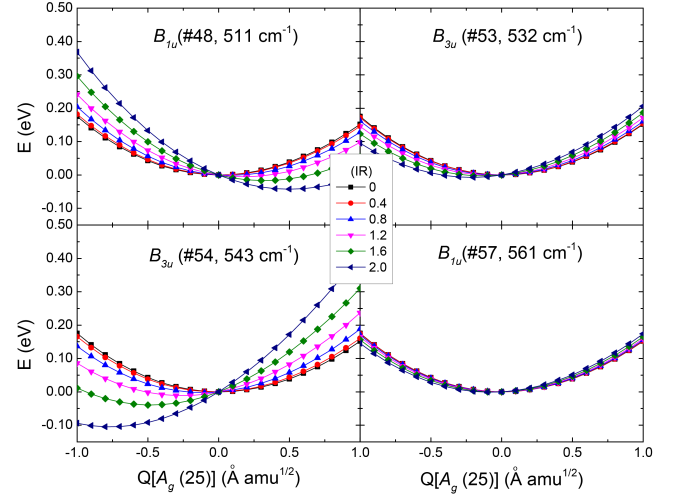


FIG. 2. Energy profiles for the nonlinear coupling between an IR-active mode and the $A_g(25)$ mode.

Raman $A_g(25)$ mode and five B_u IR-active modes with the highest frequencies are examined. (The frequencies and phonon characters for the five IR modes are given in Ref. 28). By fitting the energy surfaces $E(Q_R, Q_{IR})$ to Eq. 2, we estimated the coupling coefficients g , listed in TABLE SII. We find three IR modes that have a nonlinear coupling coefficient larger than $0.01 \text{ eV}/(\text{\AA}\sqrt{\text{amu}})^3$. The energy profiles between each of these three modes and the $A_g(25)$ mode are plotted in Figure 2. When the B_{1u} mode (index no. 48, $\nu = 511 \text{ cm}^{-1}$) is pumped to an amplitude of $2 \text{\AA}\sqrt{\text{amu}}$, the $A_g(25)$ mode finds its energy minimum at a non-equilibrium position $Q(A_g) \sim 0.5 \text{\AA}\sqrt{\text{amu}}$. With the excitation of the B_{3u} mode (index no. 53, $\nu = 532 \text{ cm}^{-1}$), the energy minimum of the $A_g(25)$ mode is displaced by $\sim -0.2 \text{\AA}\sqrt{\text{amu}}$. A similar strength excitation of another B_{3u} mode (index no. 54, $\nu = 543 \text{ cm}^{-1}$) displaces the energy minimum by $\sim -0.8 \text{\AA}\sqrt{\text{amu}}$. Among these three IR modes, the nonlinear coupling coefficient for the $B_{1u}(48)$ and the $B_{3u}(54)$ are comparable. However, only the $B_{1u}(48)$ mode shifts the energy minimum of the $A_g(25)$ mode towards a larger amplitude, which is required to *reduce* the octahedral rotation angles and drive the magnetic transition. Therefore, this IR mode is selected to drive changes in the Raman mode through the NLP interaction. Note that the coefficient $g[A_g(25), B_{1u}(48)] \sim -0.039 \text{ eV}/(\text{\AA}\sqrt{\text{amu}})^3$, which is three times larger in magnitude compared to the nonlinear phononic coupling strength in LaTiO_3 . [31] This value is approximately one order of magnitude smaller than that reported in the $\text{YBa}_2\text{Cu}_3\text{O}_7$ [32] and about half of that in PrMnO_3 [18].

We compute the time evolution of the phonon modes during this process by solving the equations of motion expressed in Eq. S1 of Ref. 28. For efficient mode pumping, the laser frequency should be in a resonant condition with the IR mode. Note that it is important to consider the

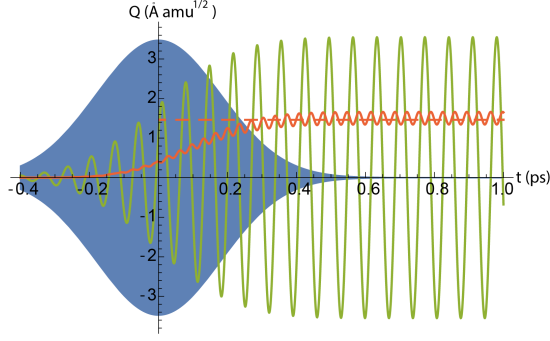


FIG. 3. (Color online) Time evolution of the A_g (25) mode (red) and the B_{3u} (48) mode (green). The laser pulse envelope is schematically shown as the blue filled-curve. The dashed line denotes the displacive vibrational center of the A_g (25) mode after pumped by a laser pulse with $\omega = 14.5$ THz and $I = 18$ MV/cm (without considering damping).

red-shift of the IR mode in the nonlinear process under high laser intensity [32]; therefore, we propose the laser frequency of 14.5 THz. With a laser intensity of 18 V/cm, the time evolution of the A_g (25) and B_{1u} (48) modes are plotted in Figure 3. The maximum displacement of the A_g (25) mode is $\sim 1.5 \text{ Å}\sqrt{\text{amu}}$ corresponding to a rotational angle reduction of $\sim 2.7^\circ$. When we compare this value to the estimated critical angle from Figure 1, $\Delta\phi(\text{FM}/\text{A-AFM}) = -4.4^\circ$ and $\Delta\phi(\text{A-AFM}/\text{G-AFM}) = -5^\circ$, we find the octahedral rotation angle reduction is of the same order, but only 60% of that required to induce the magnetic transition. The above simulation suggests that a laser pump with the intensity of 18 MV/cm is insufficient to drive the transition. In order to dynamically achieve the magnetic phase transition, one should then either increase the laser intensity or reduce the critical rotation angle through additional means. We discuss both options next.

Figure 4 shows the stationary non-equilibrium displacements (damping is neglected in our discussion) of the A_g (25) mode as a function of the laser intensity at different pump frequencies. We find that at low laser intensity, a higher frequency pump induces a larger displacive amplitude of the Raman mode whereas lower pump frequencies lead to larger maximum displacements. There is also a change in the displacive Raman amplitude with respect to the laser intensity, which indicates the dominate factors in the low-intensity condition and the high-intensity conditions are different.

This behavior can be understood by considering the renormalization of the frequency of the IR mode [32]. At low-laser intensity, the renormalized frequency of the IR mode is close to that of its eigenfrequency, $\tilde{\nu}_{IR} \approx \nu_{IR}$. Then the pumped IR amplitude, as well as the driven displacive Raman amplitude, increase proportionally to the laser intensity. However, in the high intensity limit, the renormalized frequency of the IR mode is red-shifted

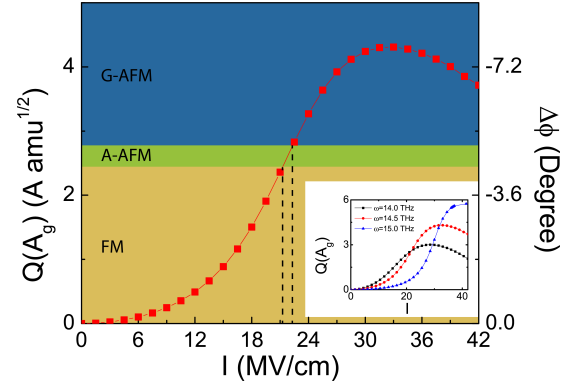


FIG. 4. (Color online) Mode amplitude $Q(A_g)$ and the change in rotation angle $\Delta\phi$ as a function laser intensity. Different colors denote different magnetic order, according to that in Fig. 1. The inset shows the same quantity for different pump frequencies.

according to the nonlinear coupling. When the renormalized IR frequency $\tilde{\nu}_{IR}$ is close to the pump laser frequency, the IR mode is pumped resonantly, which dramatically increases the mode amplitude. In this case, beating-type vibrational dynamics result between the IR and the Raman mode with the maximum displacive Raman mode found at resonance. Because the resonant condition is reached at a higher pump intensity for a lower pump laser frequency, the maximum Raman amplitude is then larger than that induced by a higher pump frequency.

Although one can increase the laser intensity to acquire a larger displacive Raman mode, the laser damage threshold of the material limits the largest laser intensity that can be used in the pump-probe experiment [33]. Also, heating of the sample due to an intense laser pulse is problematic for low-temperature measurements—here the experiments should be performed below the bulk magnetic ordering temperatures of the titanates. A more practical way to experimentally observe the dynamical phonon-induced magnetic phase transition is to reduce the critical rotation angle required for the phase transition.

Here we propose to impose static epitaxial strain on a YTO thin film grown on a [110]-oriented substrate. This mechanical constraint is based on the fact that both the rotation and tilt angle should be reduced to bring the material close to the phase transition point. If the sample is strained in the usual [001] substrate orientation, the changes in the rotation and the tilt angles have an opposite trend and effectively cancel one another: For compressive (tensile) strains, the rotation angle increases (decreases) while the tilt angle decreases (increases). If the sample is grown on a [110]-oriented substrate, and strain is applied along (111) and $(\bar{1}\bar{1}1)$ direction (in terms of pseudo-cubic coordinates), then both the rotation and tilt angles will decrease or increase together [34]. Indeed for YTO, we find both angles decrease almost linearly when tensile strain is applied [28]. The energy difference between the

FM and G -AFM phase is only 0.4 meV/f.u. at a tensile strain of 2%, suggesting a substrate lattice constant of approximately 3.98Å would be the best option. This features make KTaO_3 ($a \sim 3.988\text{\AA}$) a good candidate for which to grown YTO thin films upon and attempt the magnetophononic experiment.

Another possible route to reduce the critical rotation angle is to consider the excitation of a Jahn-Teller (JT) type Raman mode. The JT mode is usually closely related to the orbital occupancy and magnetic ordering in perovskites [35] and therefore could dynamically bring the system closer to the phase transition boundary. Such JT mode should be simultaneously excited through the nonlinear phononic coupling when symmetry allowed.

The authors thank M. Fechner, R. Averitt, V. Gopalan, and D. Puggioni for fruitful discussions. M.G. and J.M.R. acknowledge financial support from the U.S. Department of Energy (DOE) under Grant No. DE-SC0012375.

* jrondinelli@northwestern.edu

- [1] M. Först, R. Mankowsky, and A. Cavalleri, “Mode-selective control of the crystal lattice,” *Accounts of Chemical Research* **48**, 380–387 (2015).
- [2] Matteo Rini, Ra’anan Tobey, Nicky Dean, Jiro Itatani, Yasuhide Tomioka, Yoshinori Tokura, Robert W. Schoenlein, and Andrea Cavalleri, “Control of the electronic phase of a manganite by mode-selective vibrational excitation,” *Nature* **449**, 72–74 (2007).
- [3] M. Mitrano, A. Cantaluppi, D. Nicoletti, S. Kaiser, A. Perucchi, S. Lupi, P. Di Pietro, D. Pontiroli, M. Ricco, S. R. Clark, D. Jaksch, and A. Cavalleri, “Possible light-induced superconductivity in K_3C_{60} at high temperature,” *Nature* **530**, 461–464 (2016).
- [4] R. Mankowsky, A. Subedi, M. Först, S. O. Mariager, M. Chollet, H. T. Lemke, J. S. Robinson, J. M. Glowacki, M. P. Minitti, A. Frano, M. Fechner, N. A. Spaldin, T. Loew, B. Keimer, A. Georges, and A. Cavalleri, “Non-linear lattice dynamics as a basis for enhanced superconductivity in $\text{YBa}_2\text{Cu}_3\text{O}_{6.5}$,” *Nature* **516**, 71–73 (2014).
- [5] R. Mankowsky, A. von Hoegen, M. Först, and A. Cavalleri, “Ultrafast reversal of the ferroelectric polarization,” *Phys. Rev. Lett.* **118**, 197601 (2017).
- [6] N. A. Spaldin, D. M. Juraschek, M. Fechner, “Ultrafast structure switching through nonlinear phononics,” *Physical Review Letters* **118**, 054101 (2017).
- [7] Satadeep Bhattacharjee, Eric Bousquet, and Philippe Ghosez, “Engineering multiferroism in CaMnO_3 ,” *Physical Review Letters* **102**, 117602 (2009).
- [8] C. N. R. Rao, Asish K. Kundu, Md Motin Seikh, and L. Sudheendra, “Electronic phase separation in transition metal oxide systems,” *Dalton Transactions*, 3003–3011 (2004).
- [9] Mingqiang Gu, Qiyun Xie, Xuan Shen, Rubin Xie, Jianli Wang, Gang Tang, Di Wu, G. P. Zhang, and X. S. Wu, “Magnetic ordering and structural phase transitions in a strained ultrathin $\text{SrRuO}_3/\text{SrTiO}_3$ superlattice,” *Physical Review Letters* **109**, 157003 (2012).
- [10] June Hyuk Lee, Lei Fang, Eftihia Vlahos, Xianglin Ke, Young Woo Jung, Lena Fitting Kourkoutis, Jong-Woo Kim, Philip J. Ryan, Tassilo Heeg, Martin Roeckerath, Veronica Goian, Margitta Bernhagen, Reinhard Uecker, P. Chris Hammel, Karin M. Rabe, Stanislav Kamba, Jürgen Schubert, John W. Freeland, David A. Muller, Craig J. Fennie, Peter Schiffer, Venkatraman Gopalan, Ezekiel Johnston-Halperin, and Darrell G. Schlom, “A strong ferroelectric ferromagnet created by means of spin-lattice coupling,” *Nature* **466**, 954–958 (2010).
- [11] S. Wall, D. Prabhakaran, A. T. Boothroyd, and A. Cavalleri, “Ultrafast coupling between light, coherent lattice vibrations, and the magnetic structure of semicovalent LaMnO_3 ,” *Physical Review Letters* **103**, 097402 (2009).
- [12] M. Fechner, A. Sukhov, L. Chotorlishvili, C. Kenel, J. Berakdar, and N. A. Spaldin, “Magnetophononics: ultrafast spin control through the lattice,” *ArXiv e-prints* (2017), [arXiv:1707.03216 \[cond-mat.str-el\]](https://arxiv.org/abs/1707.03216).
- [13] Dominik M. Juraschek, Michael Fechner, Alexander V. Balatsky, and Nicola A. Spaldin, “Dynamical multiferroicity,” *Phys. Rev. Materials* **1**, 014401 (2017).
- [14] Dominik M. Juraschek and Nicola A. Spaldin, “Sounding out optical phonons,” *Science* **357**, 873–874 (2017), <http://science.sciencemag.org/content/357/6354/873.full.pdf>.
- [15] James M. Rondinelli, Steven J. May, and John W. Freeland, “Control of octahedral connectivity in perovskite oxide heterostructures: An emerging route to multifunctional materials discovery,” *MRS Bulletin* **37**, 261–270 (2012).
- [16] T. F. Nova, A. Cartella, A. Cantaluppi, M. Först, D. Bossini, R. V. Mikhaylovskiy, A. V. Kimel, R. Merlin, and A. Cavalleri, “An effective magnetic field from optically driven phonons,” *Nat Phys* **13**, 132–136 (2017).
- [17] Xin Huang, Yankun Tang, and Shuai Dong, “Strain-engineered a-type antiferromagnetic order in YTiO_3 : A first-principles calculation,” *Journal of Applied Physics* **113**, 17E108 (2013), <http://dx.doi.org/10.1063/1.4793644>.
- [18] Alaska Subedi, Andrea Cavalleri, and Antoine Georges, “Theory of nonlinear phononics for coherent light control of solids,” *Phys. Rev. B* **89**, 220301 (2014).
- [19] E. Pavarini, A. Yamasaki, J. Nuss, and O. K. Andersen, “How chemistry controls electron localization in $3d^1$ perovskites: a wannier-function study,” *New Journal of Physics* **7**, 188 (2005).
- [20] Y. Okimoto, T. Katsufuji, Y. Okada, T. Arima, and Y. Tokura, “Optical spectra in $(\text{La},\text{Y})\text{TiO}_3$: Variation of mott-hubbard gap features with change of electron correlation and band filling,” *Physical Review B* **51**, 9581–9588 (1995).
- [21] J. P. Goral and J. E. Greedan, “The magnetic structures of LaTiO_3 and CeTiO_3 ,” *Journal of Magnetism and Magnetic Materials* **37**, 315–321 (1983).
- [22] J. E. Greedan, “The rare earth-titanium (iii) perovskite oxides: An isostructural series with a remarkable variation in physical properties,” *Journal of the Less Common Metals* **111**, 335–345 (1985).
- [23] B. Keimer, D. Casa, A. Ivanov, J. W. Lynn, M. v Zimmermann, J. P. Hill, D. Gibbs, Y. Taguchi, and Y. Tokura, “Spin dynamics and orbital state in LaTiO_3 ,” *Physical Review Letters* **85**, 3946–3949 (2000).
- [24] Masahito Mochizuki and Masatoshi Imada, “Orbital-spin structure and lattice coupling in RTiO_3 where $\text{R}=\text{La},\text{P},\text{Nd}$, and Sm ,” *Phys. Rev. Lett.* **91**, 167203 (2003).
- [25] Masahito Mochizuki and Masatoshi Imada, “Magnetic and

- orbital states and their phase transition of the perovskite-type Ti oxides: Strong coupling approach,” *Journal of the Physical Society of Japan* **70**, 1777–1789 (2001).
- [26] Masahito Mochizuki and Masatoshi Imada, “Origin of g-type antiferromagnetism and orbital-spin structures in LaTiO_3 ,” *Journal of the Physical Society of Japan* **70**, 2872–2875 (2001).
- [27] Xin Huang, Yankun Tang, and Shuai Dong, “Strain-engineered a-type antiferromagnetic order in ytio_3 : A first-principles calculation,” *Journal of Applied Physics* **113**, 17E108 (2013), <http://dx.doi.org/10.1063/1.4793644>.
- [28] See Supplemental Material at [URL will be inserted by publisher] for auxiliary methodology details, structural information, linear and nonlinear phononic properties, and strain effects.
- [29] A. T. Zayak, X. Huang, J. B. Neaton, and Karin M. Rabe, “Structural, electronic, and magnetic properties of SrRuO_3 under epitaxial strain,” *Physical Review B* **74**, 094104 (2006).
- [30] R. Mankowsky, M. Frst, T. Loew, J. Porras, B. Keimer, and A. Cavalleri, “Coherent modulation of the $\text{YB}_2\text{Cu}_3\text{O}_{6+x}$ atomic structure by displacive stimulated ionic Raman scattering,” *Physical Review B* **91**, 094308 (2015).
- [31] Mingqiang Gu and James M. Rondinelli, “Role of orbital filling on nonlinear ionic raman scattering in perovskite titanates,” *Phys. Rev. B* **95**, 024109 (2017).
- [32] M. Fechner and N. A. Spaldin, “Effects of intense optical phonon pumping on the structure and electronic properties of yttrium barium copper oxide,” *Phys. Rev. B* **94**, 134307 (2016).
- [33] Mingqiang Gu and James M. Rondinelli, “Ultrafast band engineering and transient spin currents in antiferromagnetic oxides,” *Scientific Reports* **6**, 25121 (2016).
- [34] James M. Rondinelli and Nicola A. Spaldin, “Structure and properties of functional oxide thin films: Insights from electronic-structure calculations,” *Advanced Materials* **23**, 3363–3381 (2011).
- [35] H. Sawada, Y. Morikawa, K. Terakura, and N. Hamada, “Jahn-teller distortion and magnetic structures in LaMnO_3 ,” *Phys. Rev. B* **56**, 12154–12160 (1997).